Developing phages with a versatile end-label toward a model system for endocytosis*

Changyuan Wang,† Raymond Adkins,‡ and Zvonimir Dogic§
Physics Department, University of California, Santa Barbara
(Dated: September 30, 2022)

I. INTRODUCTION

Membranes are versatile materials due to their ability to easily change shape to form flat sheets or closed vesicles [1]. Plasma membranes, which exist in cells as lipid bilayers, are crucial to activities such as endocytosis and exocytosis which deliver nutrients into the cells and carry waste out of the cells [2–4]. To accomplish this, the cell membranes need to wrap around particles and bud off into a new vesicle, which protects substances from extracellular matrices and helps transport them to neighboring cells [3]. In particular, viruses like AdV 2, a kind of non-oncogenic adenovirus, enter the cell by first being enveloped by the membrane [5]. Artificial membranes are commonly used for drug delivery, carrying cargo like chemotherapeutic agents for cystic fibrosis [4, 6]. Producing these synthetic vesicles also requires closing a flat surface around cargo [2, 7–9]. A common production procedure is to assemble a monolayer emulsion droplet with enclosed drugs and force the droplet through a lipid-stabilized interface. Then the interface bends around the droplet, generating a bilayer vesicle [8–12]. Researchers may change membrane architectures according to their needs, and send them to target positions in human bodies.

Modeling these shape transformations relies on the Helfrich Hamiltonian, a well-established theoretical model for membrane physics [13–15]. The Helfrich Hamiltonian has been shown to agree with membrane systems which are both of biological and synthetic origin [3, 6, 16–18]. A simplified version of this Hamiltonian contains only bending and edge tension terms:

$$E = \int_{membrane} dA \{\frac{1}{2}\kappa K^2 + \bar{\kappa} K_G\} + \oint_S dS\, \gamma \quad (1)$$

where K is the mean curvature, K_G is the Gaussian curvature, and γ is the line tension. It can be used to predict curvature penalties during shape changes like endocytosis [3, 16]. However, lipid bilayers are nanometer-scale in thickness, and shape transformations occur too quickly and on a too small scale to be captured by optical microscopes. We cannot take high temporal and spatial resolution pictures to record the changes, let alone extract curvatures over time from the images [5, 19]. Thus, experimental resolution in conventional lipid bilayers during events like wrapping is insufficient to see if they match theoretical predictions.

To remedy this, we use colloidal rods, consisting of the bacteriophage M13, to form a monolayer membrane. These membranes are about 1 μm in thickness, and their dynamics occur on minutes- to hours-long timescales, where optical microscopes can easily record their shape change, visualizing the entire process, and measuring relevant physics parameters, such as curvature, bending constants, diffusion rates, etc [20–22].

II. COLLOIDAL PHAGE MEMBRANE

As the name of the colloidal phage monolayer suggests, its building blocks are filamentous bacteriophages. Phages are rod-like viruses consisting of circular single-stranded DNA enveloped by major and minor coat proteins [23]. Five minor proteins, called the P3 coat protein, protrude out and can serve as binding sites for end-labeling the phages.

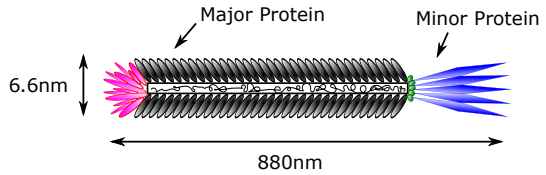

FIG. 1: A schematic diagram of M13 (not drawn to scale). It has a length of about 880 nm and a diameter of about 6.6 nm. M13 comprises a sequence of DNA with major coat proteins enveloped around it and with minor proteins sticking out at the ends [24].

Phages are highly monodisperse, meaning that every phage has the same length, which is set by the

* Kindly funded by Worster Family
† Undergraduate Researcher
‡ Graduate Mentor
§ Principal Investigator

length of the DNA packaged inside of it [25]. M13, a naturally existing phage, is one of the most common filamentous phages in display studies [24, 26]. A schematic diagram of M13 is illustrated in figure 1.

Phages can spontaneously form membranes by a self-assembly process [26–28]. To prepare a membrane sample, free-floating phage particles are suspended in solutions with salt and the depleting polymer Dextran (concentrations: 40mg/ml Dextran and 100mM salt in figure 2 case). Under these conditions, phages will assemble into the membrane phase over the course of several hours [22, 26]. Salt acts to screen the negatively charged phages, reducing the electrostatic force that repels phages away from each other. The depleting polymers exert an entropic interaction that provides an attractive force to balance the repulsive electrostatic force [22, 28]. This causes phages to come together at a distance associated with an energy minimum, forming membranes that look like disks shown in figure 2.

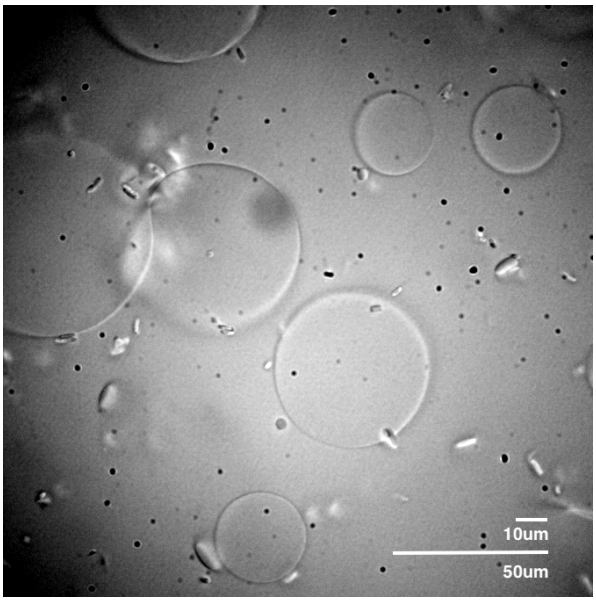

FIG. 2: A top view of the M13C7C membrane under differential interference contrast microscopy (DIC). The flat disks are M13C7C membranes with diameters of about 50 μm.

Many kinds of phages can make membranes like the ones in figure 2. With the goal to study shape change, we must find phages with versatile end tags. The minor proteins of wild-type phages do not have an end tag, but mutants can be made which have labeled ends [26, 29]. By genetically engineering their DNA sequence we can acquire phages with different lengths and end proteins [29, 30]. Therefore, we can deliberately tune the DNA of wild-type phages to realize specific end tags.

M13C7C, as shown in figure 2, is one of such genetically engineered mutants of M13. It has the same diameter, stiffness, and charge as M13, but has different minor proteins [29, 30]. M13C7C has two cysteines at the terminus of the P3 coat protein, separated by seven random amino acids [30]. The thiols in the cysteines are functional groups that can conveniently react with many chemicals, so diverse molecules can be attached to M13C7C's ends, to allow for end labeling [31–33].

III. END LABELING

A. Materials and Methods

Maleimide is a chemical compound that reacts with the thiol groups, like those found on M13C7C's ends with high efficiency. Thiol-maleimide reaction is a well-known click chemistry [31, 32], meaning that this conjugation is fast, convenient, highly specific, and the yield is satisfactory [33]. However, we must still ensure that this chemistry works in our system. When the two cysteines on M13C7C are exposed to oxygen, a disulfide bridge will form. Consequently, after M13C7C is grown and purified using standard preparation protocol [29, 34], any subsequent reactions should take place in degassed solutions to avoid oxygen [29].

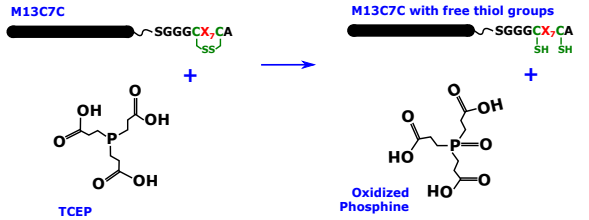

FIG. 3: A simplified schematic diagram of how TCEP opens the loop on M13C7C ends, creating two free thiol groups [29, 35]. C stands for cysteine, X_7 stands for the 7 random amino acids between two cysteines.

To attain free thiols, we introduce a reducing agent tris(2-carboxyethyl)phosphine hydrochloride (TCEP, Thermo Scientific) around 2mM to break the disulfide bond [29, 36, 37]. As figure 3 suggests, thiol groups should be available after hitting with TCEP for 48 hours [29].

However, maleimide cannot be added directly afterward. As the chemistry in figure 4 shows, TCEP reacts with maleimide. Thus, before we add maleimide, an extra step of dialyzing out excessive TCEP is necessary. This is done by five rounds of

dialysis for 10 minutes each, under an inert nitrogen environment.

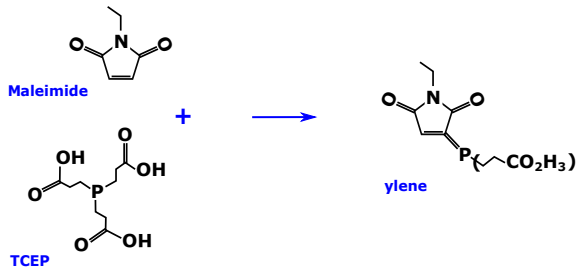

FIG. 4: A simplified schematic diagram of how TCEP reacts with maleimide, and forms remarkably stable ylenes [35].

After we ensure that no free TCEP is in the solution, the thiol-maleimide reaction can occur. We allow the chemical reaction in figure 5 to last for two hours, a time which we have found to be critical for successful conjugation. After several hours, most free thiols will be occupied, but excess unreacted maleimides are still in solution, and now begin to bind with the free amine groups in the other coat proteins surrounding the phages. At pH 6.5, the amine-maleimide reaction is about 1000 times slower than the thiol-maleimide reaction, but if all thiol sites are occupied, maleimides will still stick on phages indiscriminately [32, 38, 39]. Therefore, it is necessary to allow the reaction to proceed and then quench as soon as possible.

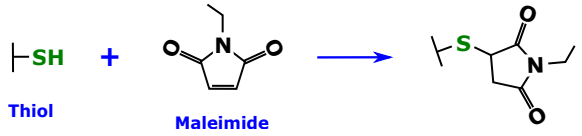

FIG. 5: A simplified schematic diagram of thiol-maleimide reaction. Each of the free thiol groups on M13C7C binds at the maleimide C=C bond [31, 32].

For example, figure 6 illustrates the lateral views of phages. In (a), the reaction proceeds for two days, so the maleimide-dye complex binds all along the phages, covering both the major and minor protein coats with dye. It means molecules that are meant to be labeled only at the ends are attached everywhere. Since the maleimide-dye molecule is small, membranes can still assemble as usual. However, we will not have specific end labeling.

Limiting the reaction time to two hours resolves the problem. Figure 6 (b) gives two noticeable bright bands in lateral perspective. Since the orientations of phages are random, the end proteins may distribute on either side of the membranes, so there are two bands instead of one.

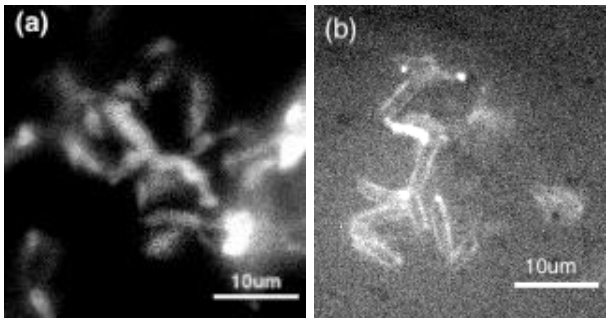

FIG. 6: Lateral views of clusters of M13C7C membranes under DIC microscopy. (a) Membranes made of phages that react with maleimide-dye for two days. Maleimide-dye is a chemical compound with maleimide on one end and fluorescent dye on the other end. The dye sticks on the sides of phages, making the membranes bright everywhere; (b) Membranes made of phages that react with maleimide-dye for two hours. There are two apparent bright bands.

B. Bead Experiment

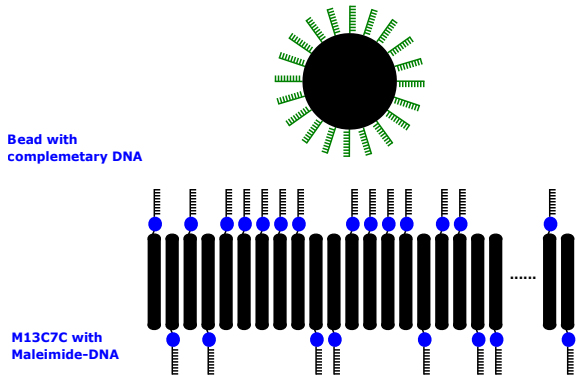

FIG. 7: A simplified schematic diagram of bead experiment. M13C7C phages labeled with maleimide-DNA form a membrane, and a bead coated with complementary strands of DNA is dropping onto the membrane. Black rods are phages; on their ends, the blue sphere represents the maleimide group. Black brushes are the DNA in maleimide-DNA, while green brushes are their complementary strands.

We have demonstrated that the thiol-maleimide reaction works well as expected, and maleimide-X particles can be successfully labeled on M13C7C ends. The next step is to switch maleimide-dye into maleimide-DNA to study shape changes during wrapping [40]. Just like what is described in the maleimide-dye demonstration, maleimide-DNA

brushes are randomly labeled on either side of the membranes. To produce a model system for membrane endocytosis, we flow in polystyrene beads coated with complementary strands of DNA. As the bead drops on the membrane, the complementary single-stranded DNA hybridizes, causing the membranes to wrap around the beads like the illustration in figure 7.

When the membrane wraps around the bead, there is an energy cost for curvature according to Helfrich Hamiltonian:

$$E_{bend} = \int_{membrane} \frac{1}{2}\kappa K^2 \, dA \tag{2}$$

κ is about 10,000 k_bT for colloidal membranes, mean curvature K is $\frac{2}{10\mu m}$ (radius of normal beads is around 10 μm), dA is the surface area of the beads, so to completely cover a bead, the curvature penalty is around 500,000 k_bT. This energy penalty is compensated for by the energy of hydrogen bonds between DNA strands, which is about 1 k_bT per base pair. The DNA we selected has 30 base pairs, so we need less than 17,000 DNA per bead to match the cost of bending energy to envelop the bead. This means that for a 10 µm bead, we require a graft density of 14 DNA per μm^2. Our collaborator Benjamin Rogers in Brandeis can achieve a graft density of more than 6000 DNA per μm^2, which is beyond sufficient for our purpose [22, 41].

We are labeling maleimide-DNA and awaiting our collaborators to make DNA-coated beads at the same time. When both the labeled phages and beads are available, we can image the dynamic transitions of how two-dimensional membranes wrap into a 3D vesicle and analyze the collected data.

This bead experiment will serve as an analogy for the wrapping and budding-off events among biological membranes. For example, after AdV 2 adenoviruses enter the cell, cell membranes enclose the virus and split off a vesicle [5]. Researchers have used TEM images to analyze the correlation between shape changes and exocytosis, but again, there is no data on time evolution [5, 8, 42]. The bead experiment can serve as a model for the entire process. Lipid bilayers are 10 nm in thickness and wrap around viruses which are 100 nm in diameter [43]. By comparison, phage membranes are about 1 μm in thickness, so 10 μm beads match the relative scale of membrane thickness to particle size. Since our membranes are 100 times thicker, we can easily visualize the changes and get high-resolution videos in both space and time.

IV. CONCLUSION AND FUTURE WORK

In conclusion, phage monolayers are a functional model system to study membrane shape changes. It provides insights into biological membrane deformations like exocytosis as well. Other than wrapping, spontaneous curvature is also a common phenomenon among lipid bilayers in living cells [1, 14]. Some proteins and lipids, like cholesterol, occasionally land on membranes or are embedded into membranes, creating asymmetries concerning two sides of the membranes [44, 45]. The difference in molecular structures drags the system away from equilibrium [3], so to achieve the highest entropy and lowest energy, membranes transform into curved configurations. As we have mentioned, any shape change is challenging to investigate in a time series for conventional biological membranes. Spontaneous curvature, which relates to curving, is not an exception. Phage monolayers can again solve this problem. After assembling the colloidal membrane with single-stranded DNA like figure 7 shows, we can flow in large molecules with a complementary strand of DNA. As two strands of DNA hybridize, membranes will curve correspondingly to maximize entropy. This process is an analogy to the landing of particles on a biological membrane.

The main concern is that the orientation of phages is difficult to control. If target particles flow into the sample, they may bind to the DNA on either side of the membranes at any location. It is better to have molecules sitting on only one side of the membranes, so bead envelopment is easier to be measured and analyzed. Substituting 2D membranes with 3D vesicles can achieve this goal. Then the floating molecules can then only contact the exterior surfaces. However, the usual sizes of M13C7C membranes are too small to bend into a sphere, so it is necessary to look for other types of phages. Litmus, a 380 nm phage, makes decent vesicles in previous experiments. However, their end proteins have less than 10% labeling efficiency. Such low efficiency is usually hard to detect under optical microscopes. One possible approach is to transform the DNA sequence that controls the end proteins of M13C7C into litmus which is a work that is currently in progress [46, 47]. End proteins are too small to affect the general properties of phages [30], so the new litmus-C7C, the litmus phage with the end proteins of M13C7C, should be an approximately 380 nm phage with seven random amino acids flanked by cysteines at the end. The litmus-C7C will then make vesicles with efficient end binding sites, which we will use to perform experiments and collect data from.

ACKNOWLEDGMENTS

I would like to thank the generous support of the Worster family. They kindly funded me to be fully dedicated to the research with no financial burden over the summer. I also want to express my gratitude towards my PI Zvonimir Dogic, and my graduate mentor Raymond Adkins. They guided me along the way, illuminating possible directions when I was stuck in experiments. I would not accomplish this end-labeling project without them. The Worster committee, other mentors, and mentees in the biweekly meetings also rendered practical feedback that helped to polish my work.

[1] M.M. Kozlov, *Physics of Biological Membranes* (Springer, 2018) pp. 287–309.

[2] Marcel Mulder, *Basic principles of membrane technology*, 2nd ed. (Springer Dordrecht, 1996).

[3] Thomas Schubert and Winfried Römer, "How synthetic membrane systems contribute to the understanding of lipid-driven endocytosis," Biochimica et Biophysica Acta (BBA) - Molecular Cell Research **1853**, 2992–3005 (2015).

[4] Harden M. McConnell and Roger D. Kornberg, "Inside-outside transitions of phospholipids in vesicle membranes," Biochemistry **10**, 1111–1120 (1971).

[5] Thorley JA, McKeating JA, Rappoport JZ, "Mechanisms of viral entry: sneaking in the front door," Protoplasma **244**, 15–24 (2010).

[6] Davis AP, Sheppard DN, Smith BD, "Development of synthetic membrane transporters for anions," Chemical Society Reviews **36**, 348–357 (2007).

[7] Osada, Y., Nakagawa, T., *Membrane Science and Technology*, 1st ed. (New York: Marcel Dekker, 1992).

[8] Ariane Peyret, Hang Zhao, and Sébastien Lecommandoux, "Preparation and properties of asymmetric synthetic membranes based on lipid and polymer self-assembly," Langmuir **34**, 3376–3385 (2018).

[9] Martina Garni, Sagana Thamboo, Cora-Ann Schoenenberger, Cornelia G. Palivan, "Biopores/membrane proteins in synthetic polymer membranes," Biochimica et Biophysica Acta (BBA) - Biomembranes **1859**, 619–638 (2017).

[10] A. Boker P. van Rijn, M. Tutus, C. Kathrein, L. Zhu, M. Wessling, U. Schwaneberg, "Challenges and advances in the field of self-assembled membranes," Chemical Society Reviews **42**, 6578–6592 (2013).

[11] D.M. Vriezema, M. Comellas Aragonès, J.A.A.W. Elemans, J.J.L.M. Cornelissen, A.E. Rowan, R.J.M. Nolte, "Self-assembled nanoreactors," Chemical Reviews **105**, 1445–1490 (2005).

[12] D.E. Discher, F. Ahmed, "Polymersomes," Annual Review of Biomedical Engineering **8**, 323–341 (2006).

[13] Markus Deserno, "Fluid lipid membranes – a primer," (2006).

[14] W. Helfrich, "Elastic properties of lipid bilayers: Theory and possible experiments," Zeitschrift für Naturforschung Cs **28**, 693–703 (1973).

[15] Argudo D , Bethel NP, Marcoline FV, Grabe M, "Continuum descriptions of membranes and their interaction with proteins: Towards chemically accurate models," Biochimica et Biophysica Acta **1858**, 1619–1634 (2016).

[16] Agrawal, Himani, Liu, Liping, and Sharma, Pradeep, "Revisiting the curvature-mediated interactions between proteins in biological membranes," Soft Matter **12**, 8907–8918 (2016).

[17] Argudo D, Bethel NP, Marcoline FV, Grabe M, "Continuum descriptions of membranes and their interaction with proteins: Towards chemically accurate models," Biochimica et Biophysica Acta **1858**, 1619–1634 (2016).

[18] Farago O, Pincus P, "Statistical mechanics of bilayer membrane with a fixed projected area," The Journal of Chemical Physics **120**, 2934–2950 (2004).

[19] Morgan Chabanon, James C.S. Ho, Bo Liedberg, Atul N. Parikh, Padmini Rangamani, "Pulsatile lipid vesicles under osmotic stress," Biophysical Journal **112**, 1682–1691 (2017).

[20] Sharma, P., Ward, A., Gibaud, T. et al, "Hierarchical organization of chiral rafts in colloidal membranes," Nature **513**, 77–80 (2014).

[21] Edward Barry and Zvonimir Dogic, "Entropy driven self-assembly of nonamphiphilic colloidal membranes," Proceedings of the National Academy of Sciences **107**, 10348–10353 (2010).

[22] Balchunas, Andrew J., Cabanas, Rafael A., Zakhary, Mark J., Gibaud, Thomas, Fraden, Seth, Sharma, Prerna, Hagan, Michael F., and Dogic, Zvonimir, "Equation of state of colloidal membranes," Soft Matter **15**, 6791–6802 (2019).

[23] Roux, S., Krupovic, M., Daly, R.A. et al, "Cryptic inoviruses revealed as pervasive in bacteria and archaea across earth's biomes," Nature Microbiology **4**, 1895–1906 (2019).

[24] Hyo-Eon Jin, Woo-Jae Chung, and Seung-Wuk Lee, *Research Methods in Biomineralization Science*, 2nd ed. (Academic Press, 2013) pp. 305–323.

[25] Seung-Wuk Lee, Chuanbin Mao, Christine E. Flynn, and Angela M. Belcher, "Ordering of quantum dots using genetically engineered viruses," Science **296**, 892–895 (2002).

[26] Zvonirmir Dogic, "Filamentous phages as a model system in soft matter physics," frontiers in Microbiology - Virology **7** (2016).

[27] Yang SH, Chung WJ, McFarland S, Lee SW, "Assembly of bacteriophage into functional materials," The Chemical Record **13**, 43–59 (2013).

[28] Thomas Gibaud, "Filamentous phages as building blocks for reconfigurable and hierarchical self-assembly," Journal of Physics: Condensed Matter

29 (2017), 10.1088/1361-648X/aa97f9.

[29] Alexis de la Cotte, Cheng Wu, Marie Trévisan, Andrii Repula, and Eric Grelet, "Rod-Like Virus-Based Multiarm Colloidal Molecules," ACS Nano **11**, 10616–10622 (2017).

[30] Andrii Repula, *Structure and dynamics of rod-like colloids with patchy interaction*, Theses, Université de Bordeaux (2019).

[31] Devatha P. Nair, Maciej Podgórski, Shunsuke Chatani, Tao Gong, Weixian Xi, Christopher R. Fenoli, and Christopher N. Bowman, "The Thiol-Michael Addition Click Reaction: A Powerful and Widely Used Tool in Materials Chemistry," Chemistry of Materials **26**, 724–744 (2014).

[32] Northrop, Brian H., Frayne, Stephen H., and Choudhary, Umesh, "Thiol–maleimide "click" chemistry: evaluating the influence of solvent, initiator, and thiol on the reaction mechanism, kinetics, and selectivity," Polymer Chemistry **6**, 3415–3430 (2015).

[33] Neal K. Devaraj and M. G. Finn, "Introduction: Click Chemistry," Chemical Reviews **121**, 6697–6698 (2021).

[34] Sambrook, J.; Russell, D. W., *Molecular Cloning: A Laboratory Manual*, 3rd ed. (Cold Spring Harbor Laboratory Press: New York, 2001).

[35] Terrence Kantner, Bayan Alkhawaja, and Andrew G. Watts, "In situ quenching of trialkylphosphine reducing agents using water-soluble peg-azides improves maleimide conjugation to proteins," ACS Omega **2**, 5785–5791 (2017).

[36] C. Rentero Rebollo, I.; Heinis, "Phage selection of bicyclic peptides," Methods (Amsterdam, Netherlands) **60**, 46–54 (2013).

[37] Bellotto, S.; Chen, S.; Rentero Rebollo, I.; Wegner, H. A.; Heinis, C., "Phage selection of photoswitchable peptide ligands," Journal of the American Chemical Society **136**, 5880–5883 (2014).

[38] Norman E. Sharpless and Martin Flavin, "The reactions of amines and amino acids with maleimides. structure of the reaction products deduced from infrared and nuclear magnetic resonance spectroscopy," Biochemistry **5**, 2963–2971 (1966).

[39] G. T. Hermanson, *Bioconjugate Techniques*, 3rd ed. (New York, 2013) pp. 229–258.

[40] Paris C, Brun O, Pedroso E, Grandas A., "Exploiting protected maleimides to modify oligonucleotides, peptides and peptide nucleic acids," Molecules **20**, 6389–6408 (2015).

[41] W. Benjamin Rogers and John C. Crocker, "Direct measurements of dna-mediated colloidal interactions and their quantitative modeling," Proceedings of the National Academy of Sciences **108**, 15687–15692 (2011).

[42] Liu J, Li W, Zhang X, Feng Y, Fang X, "Ligand-receptor binding on cell membrane: Dynamic force spectroscopy applications," Methods in Molecular Biology **1886**, 153–162 (2019).

[43] Louten J, *Essential Human Virology*, 19th ed. (Academic Press, 2016).

[44] Bartosz Różycki and Reinhard Lipowsky, "Spontaneous curvature of bilayer membranes from molecular simulations: Asymmetric lipid densities and asymmetric adsorption," The Journal of Chemical Physics **142** (2015), 10.1063/1.4906149.

[45] Hossein A, Deserno M., "Spontaneous curvature, differential stress, and bending modulus of asymmetric lipid membranes," Biophysics Journal **118**, 624–642 (2020).

[46] Sambrook, J. and Russell, D.W., *Molecular Cloning: A Laboratory Manual*, 3rd ed., Vol. 1 (Cold Spring Harbor Laboratory Press, New York, 2001).

[47] Noren, K. A., and Noren, C. J., "Construction of high-complexity combinatorial phage display peptide libraries," Methods (San Diego, Calif.) **1886**, 169–178 (2001).